Radiofrequency planar surface coil for Magnetic Resonance: when the use of a circular wire gives a noticeable advantage with respect to a flat strip conductor?

Giulio Giovannetti[1,2], Gianluigi Tiberi[3,4], Michela Tosetti[3,4], Agostino Monorchio[5,6], Nunzia Fontana[6]

[1]Institute of Clinical Physiology, National Council of Research, Pisa, Italy

[2]Fondazione G. Monasterio CNR - Regione Toscana, Pisa, Italy

[3]Laboratory of Medical Physics and Biotechnologies for Magnetic Resonance, IRCCS Stella Maris Foundation, Pisa, Italy

[4]Imago7 Foundation, Pisa, Italy

[5]Department of Information Engineering, University of Pisa, Pisa, Italy

[6]Consorzio Nazionale Interuniversitario per le Telecomunicazioni, Pisa, Italy

Abbreviated title: Circular wire and flat strip conductors for Magnetic Resonance coils

Correspondence to:

G. Giovannetti, I.F.C., C.N.R.

Via Moruzzi 1, 56124 S. Cataldo, Pisa, Italy.

E-mail: giovannetti@ifc.cnr.it

Phone: +39 050 3152827

Fax: +39 050 3152166

Abstract

Depending on their cross-sectional shape, commonly used conductors for radiofrequency (RF) Magnetic Resonance (MR) coils can be categorized into circular wires and flat strips. Due to a more symmetrical current distribution inside conductor volume, coils constituted by wire conductors provide better overall performance in unloaded conditions with respect to the ones made of strip conductor, although wire conductors are difficult to handle for coil manufacturing and additional mechanical competencies are required. Nevertheless, the accomplishment of the best coil performance during imaging, i.e. in the presence of a sample, remains the main issue in MRI. It follows that the use of wire conductors instead of strip ones is worthwhile only if the correspondent increase in coil quality factor with sample is substantial: this is related to the ratio between sample and coil resistance.

This paper proposes the application of a finite element method (FEM)-based numerical approach for separately estimating the conductor and radiative losses in planar surface loops characterized by different cross-sectional shapes (circular wire and flat strip) in conjunction with a vector potential calculation-based method for sample-induced resistance estimation. Simulation data were acquired from 5.7 to 128 MHz, for four different size loops (from 2 to 15 cm diameters), with the scope of evaluating the region in the frequency-loop diameter plane where the use of a circular wire conductor gives a noticeable advantage with respect to the flat strip in maximizing signal-to-noise ratio (SNR) in MR applications.

Keywords: numerical methods; radiofrequency coils; coil losses; sample losses; signal-to-noise ratio; Magnetic Resonance

1. Introduction

Signal-to-noise ratio (SNR) in magnetic resonance (MR) experiments is affected by the coil resistance and by the sample-induced resistance values [1]. In particular, at lower frequencies SNR

is mainly ascribed to the coil losses [2] whereas the sample losses are dominant [3] at higher frequencies, as it generally happens for 1.5 T and 3 T ^{1}H coils design.

Coil resistance strongly depends on conductor cross-sectional shape; this latter can be classified as circular rod shapes (also referred to as *circular wires*) and rectangular shapes (*flat strips*) [4]. Moreover, the radiofrequency (RF) energy loss is influenced by radiation resistance, which takes into account for the *antenna effect* [5].

In a previous work [6], authors proposed the use of finite element method (FEM)-based numerical approach for separately estimating the conductor and radiative losses in circular wire loop RF coils for different tuning frequencies (from 5.7 to 128 MHz). In a successive work [7], the same simulation approach has been employed for flat strip loops and simulation results were validated through workbench tests performed on flat strip and circular wire coil prototypes.

However such approach, since sample losses are neglected, is mainly useful when an optimal coil design is pursued by minimizing the coil noise, and it does not consider the sample noise; indeed, this last can be dominant when the sample dimensions are not small compared to the wavelength, i.e., at high field MR imaging [8].

As an example, we mention the loop-coils for MR micro-imaging, where wires are used since, in this case, the sample losses are small compared to coil ones. Moving towards clinical applications, loop coils may have larger diameters, increased sample volume and resistance, and solutions using flat strip loops can be found in the market. The use of flat strips instead of circular wire for coil loops is advantageous only if the coil quality factor increase in imaging conditions, i.e. in the presence of the sample.

Sample-induced resistance can be estimated by using a method which employs vector potential calculation (VPC), which can be easily implemented in analytical form for sample-induced resistance estimation of simple coil and sample geometries [9].

In this paper we propose the application of FEM for estimating flat strip and circular wire loop coil losses and VPC for sample-induced resistances estimation from 0.13 T to 3.0 T, i.e. from 5.7 MHz

to 128 MHz, for four different loop sizes (from 2 to 15 cm diameters), with the aim of evaluating the combination of frequency and loop diameter where the use of a circular wire gives a noticeable advantage with respect to the flat strip.

2. Materials and Methods

2.1 RLC circuit and SNR estimation

RF coil study can be approached by using an equivalent *RLC* circuit (Fig. 1), in which the current *I* is generated by *V*, alternately the voltage source (for transmitter coil) or the sample-induced voltage (for receiver coil), as according to the reciprocity theorem [10]. *L* is the system inductance which depends on conductors size and geometry and takes into account the energy stored in the magnetic field, while *C* is the system capacitance resulting from the contribution of discrete capacitors.

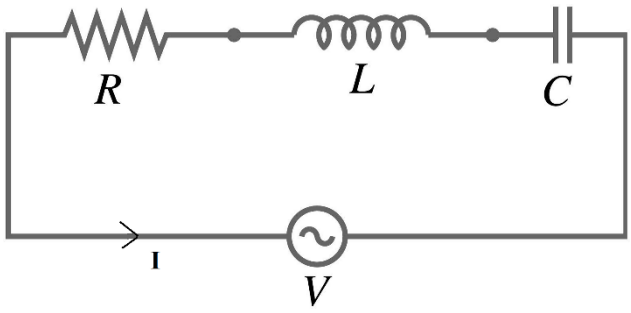

Fig. 1

Both *L* and *C* affect the circuit resonant frequency, which can be calculated as:

$$f_0 = \frac{1}{2\pi\sqrt{LC}} \tag{1}$$

The resistance *R* is the overall sum of the resistances associated with the loss mechanisms within the conductor and within the sample [11] and can be evaluated as:

$$R = R_{coil} + R_{sample} + R_{extra} \tag{2}$$

R_{coil} takes into account the losses within the coil conductors and depends on the conductor geometry, R_{sample} represents the sample losses caused by RF currents, induced by the fluctuating

magnetic field and by electric fields in the sample. Finally, the term R_{extra} indicates radiative losses (R_{irr}), tuning capacitor losses (R_{cap}) and soldering losses (R_{sold}).

A quantitative measure of coil quality factor Q can be expressed in terms of circuit parameters as [8]:

$$Q = \frac{2\pi f_0 L}{R} = \frac{1}{R}\sqrt{\frac{L}{C}} \tag{3}$$

while the sensitivity to loading can be evaluated through the ratio r between the unloaded quality factor (Q_{empty}) and the one in loaded condition (Q_{sample}) [12]:

$$r = \frac{Q_{empty}}{Q_{sample}} = 1 + \frac{R_{sample}}{R_{coil} + R_{extra}} \tag{4}$$

Generally, a coil has to be designed by minimizing the coil noise with respect to the sample noise, thus allowing to achieve the highest SNR from a given coil architecture, being $SNR \approx \sqrt{1 - \frac{1}{r}}$ [13], which can be written in terms of loss contributions by using Eq. (4) as $SNR \approx \sqrt{\frac{R_{sample}}{R_{sample} + R_{coil} + R_{extra}}}$.

2.2 Coil losses estimation by FEM

Coil losses prediction for circular wire and flat strip conductors can be achieved using a numerical method implementing the FEM algorithm, such as HFSS (Ansys, Canonsburg, PA, USA) employed in this work. A set of simulations has been perfomed investigating circular coils with different size (2, 5, 10 and 15 cm diameters) constituted by circular wire and flat strip conductors, whose sizes guarantee the same inductance between strip and wire conductors (0.1 cm radius circular wire and 4.482 mm width × 0.04 mm thickness strip) [4]. All coils were simulated as purely inductive, without tuning capacitors, in order to reduce the computation time [14], and the impedances were calculated at different frequencies (f=5.7, 21.3, 63.9 and 127.8 MHz). Lumped port (S-port), employed as feeding source, allows calculating the S parameters of the electromagnetic model

based on a defined reference impedance (50 Ω) and also allows to calculate the corresponding input impedance.

The estimated real part of the impedance corresponds to *R*, constituted by the sum of coil resistance (R_{coil}) and radiative losses (R_{irr}), which can be evaluated separately with FEM. As in the previously cited works [6, 7], the simulations have been performed using an adaptive tetrahedral mesh with an automatic convergence detection. The mesh adaptation procedure provided a minimum edge length of 9.8 μm and 8 μm for the circular wire and the flat strip coil, respectively.

2.3 Sample-induced resistance calculation with VPC

The estimation of losses associated to sample-induced resistance has been performed by using homogeneous infinitely long cylinders [15, 16], spheres [1] or half-spaces [17] as approximations of the sample geometry.

In this work, a VPC method based on the magnetostatic approach has been used. Depending on the coil geometry and shape, sample-induced resistance estimation can be performed by using [18]:

$$R_{sample} = \sigma\omega^2 \int_{vol} A * A \, dV \tag{5}$$

where σ is the sample conductivity, A is the magnetic vector potential produced by the current flowing in the coil and the integral is performed over the sample volume.

Different algorithms can be used in Eq. (5) for vector potential calculation, assessed with Legendre polynomials [19], spherical harmonics [18], surface integrals [20] and Lipschitz-Hankel integral [21]. However, all these methods are known to require convoluted calculations, whereas good accuracy can be achieved even with a simple method, which can be easily mathematically implemented.

The magnetic vector potential produced by a current flowing in a loop can be computed as [8]:

$$A(r) = \frac{\mu_0 I}{4\pi} \int_{C_C} \frac{dl}{W} \tag{6}$$

where *I* is the electric current flowing in the *C* contour, *dl* is the infinitesimal vector tangential to *C* and *W* is the distance between the observation point with (x, y, z) coordinates and the conductor path (see Fig. 2). Eq. (6) can be easily solved through Elliptic integrals [22].

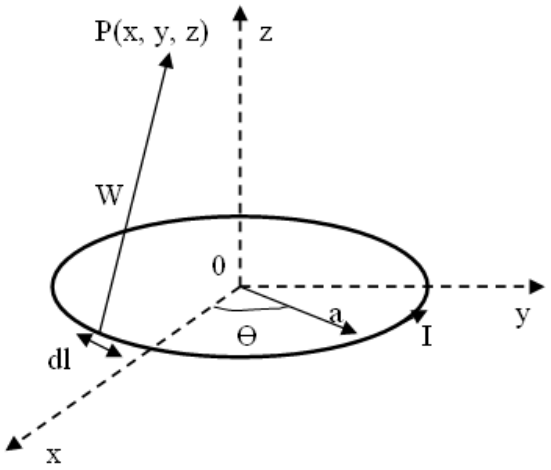

Fig. 2

2.4 Capacitance and soldering losses

It is well known that capacitor losses can reduce coil overall performance, especially for lower frequency designs. Therefore in order to obtain high-performance coils, the use of high-quality capacitors is well recommended. For achieving an estimation of capacitor losses, the inductance values of the four different size loops were calculated by using an in-house software simulator [23]; the capacitance values have been therefore calculated for tuning the coils at the four different frequencies. Finally, capacitance losses can be estimated from capacitor datasheets [24] by using the dependence of capacitor equivalent series resistance (ESR) with the frequency according to the $f^{1/2}$ law, which is the same as for the conductor skin depth losses, being ESR largely determined by the capacitor electrodes resistance [25].

Further resistive losses can be ascribed to the solder joints connecting the coil components, which can be extrapolated from literature data [26, 23].

3. Results

Coil resistances have been computed by FEM simulations while sample-induced resistances have been estimated by using Eq. (5) and integrating in a 30×30×30 cm^3 cuboid whose electrical conductivity (σ=0.39 S/m) meets the American Society for Testing and Material (ASTM) criteria for MR phantom developing [27]. The distances between the loops plane and the phantoms are equal to 5 mm for all simulations. Fig. 3 depicts the simulation setup showing the coil geometry and the simulated phantom.

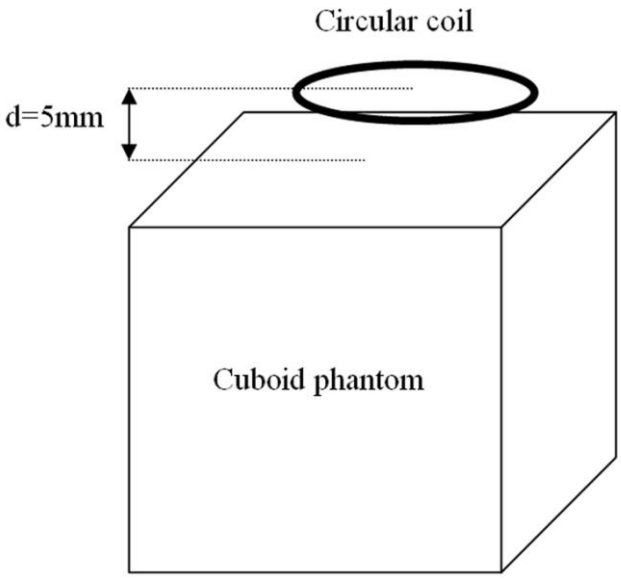

Fig. 3

Table 1, 2, 3 and 4 show different size circular wire and flat strip coil simulation results at different frequencies.

FEM simulations confirmed the higher value of losses of the coils constituted by flat strip conductor with respect to the circular wire one at all frequencies and for all coil sizes, while R_{irr} was approximately the same for flat strip and circular wire coils.

The term ΔSNR indicates the gain in SNR when using circular wire instead of flat strip, calculated as $\Delta SNR = \left(SNR_{wire} - SNR_{strip}\right) / SNR_{strip}$, being SNR estimated according to the previously

described theoretical formulation [13] and by using Eq. (4). For strip and wire coils of the same diameter, ΔSNR increase when the coils are tuned at lower frequencies, because the SNR becomes strongly dependent on the coil losses and an optimal coil design is a necessary constraint for minimizing the coil noise with respect to the sample noise.

When coil diameter diminishes, ΔSNR increases for each tuning frequency. Only for the smaller 2 cm coil the trend of the increasing ΔSNR persists only for the higher frequencies, whereas it decreases for the lower one: as a matter of fact, in the regime dominated by the coil losses, these losses begin to be comparable with those in the capacitors and soldering.

Fig. 4 summarizes the previous data by presenting them in three different regions of ΔSNR value ranges in dependence on loop diameter and frequency.

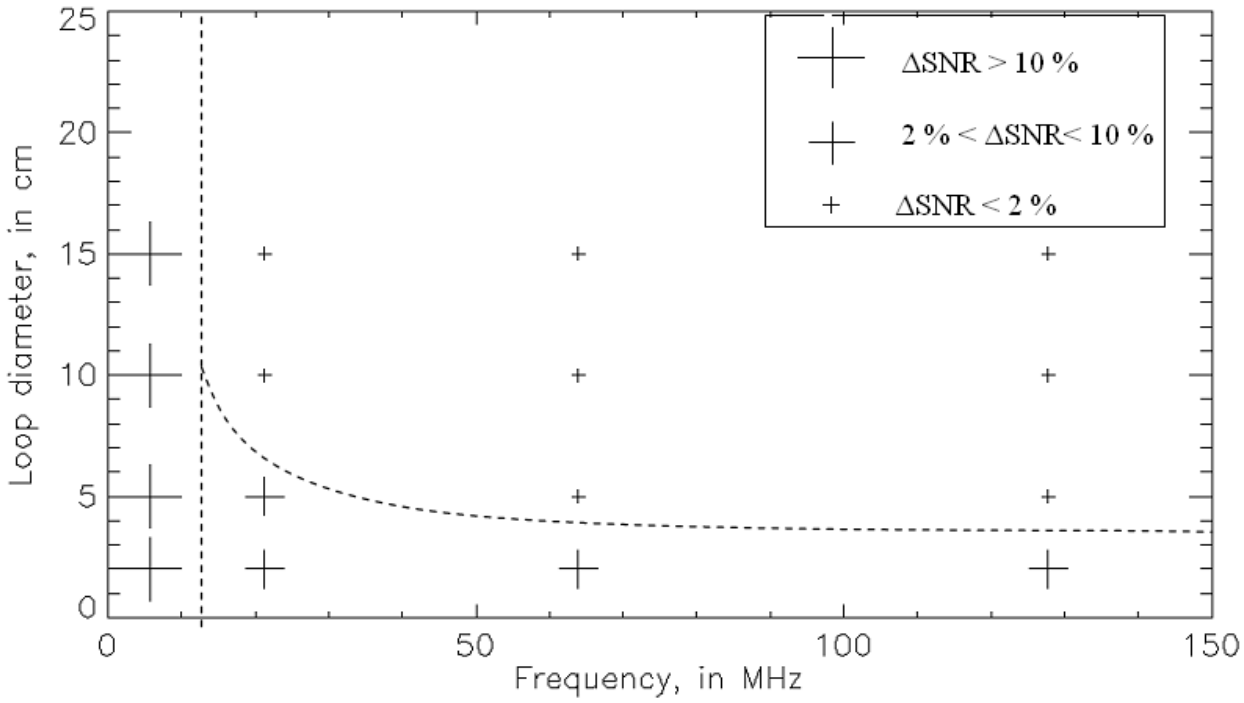

Fig. 4

4. Discussion and conclusion

This paper proposed the application of a numerical method for estimating coil losses jointly to a vector potential calculation-based method for power losses estimation in the sample.

In particular, a FEM-based numerical approach has been employed for separately estimating the conductor and radiative losses in planar surface loops characterized by different cross-sectional shapes (circular wire and flat strip). The sample-induced resistance was estimated with a different method, easily implemented in a code, because FEM would have requested an unacceptable computational time for simulating loaded coils with respect to the time guaranteed by VPC, especially for low-frequency tuned coils. Moreover, VPC approach can be properly performed when the simulated coil has a very simple geometry (e.g. circular, square or solenoidal) and the sample can be approximated by a simplified model.

The vector potential is evaluated by using quasi-static assumption, that implies a nearly static magnetic field assumption which is valid when the coil dimensions are much lower than the wavelength. This assumption is verified even at higher frequencies used in the described applications (at 128 MHz the related wavelength is 2.35 m and the nearly static assumption holds for any loop dimensions). However, its use would result in a significant error when the coil and the sample sizes are comparable to the wavelength. Both simulators have been previously validated with home-built circular coils: in particular, workbench tests for coil resistance measurements performed on two circular coil prototypes, the first one constituted by a flat strip and the second one by circular wire conductors, showed a good agreement with FEM simulations [6, 7], whereas sample-induced resistance estimation method has been validated by comparison between simulation and workbench test performed on different size coils tuned at different frequencies and loaded with a cubic sample [9].

In this work, two main issues have been addressed: 1) derive the conditions for which the sample noise dominates or is negligible with respect to the coil losses; 2) find the combination of frequencies and loop diameters where the use of a circular wire gives a noticeable advantage with respect to a flat strip. As expected, the results highlight the better performance of the coil constituted by a wire conductor with respect to the strip one in all frequency range routinely used in MR clinical scanner (5.7–128 MHz). Since a wire conductor is difficult to handle for coil

manufacturing and requires qualified mechanical personnel, for achieving a significant SNR gain we suggest using it especially when the frequency is lower or equal to 5.7 MHz for all coil diameters or for frequencies below 63.9 MHz when the loop diameter is smaller or equal to 5 cm.

References

1. D.I. Hoult, P.C Lauterbur, The sensitivity of the zeugmatographic experiment involving human samples, J Magn Reson 34 (1979), 415–433.
2. T. Claasen-Vujcic, H.M. Borsboom, H.J.G. Gaykema, T. Mehlkopf, Transverse Low-Field RF Coils in MRI, Magn. Reson. Med. 36 (1996), 111-116.
3. D.I. Hoult, R.E. Richards, The signal-to-noise ratio of the nuclear magnetic resonance experiment, J Magn Reson 24 (1976), 71–85.
4. G. Giovannetti, V. Hartwig, L. Landini, M.F. Santarelli, Low-field MR coils: comparison between strip and wire conductors, App Magn Res 39 (2010), 391-399.
5. J. Mispelter, M Lupu, A. Briguet, NMR probeheads for biophysical and biomedical experiments. London: Imperial College Press, 2015.
6. G. Giovannetti, G.L. Tiberi, M. Tosetti, Finite Element Method-based approach for radiofrequency magnetic resonance coil losses estimation, Conc Magn Reson Part B 46B (2016), 186-190.
7. G. Giovannetti, N. Fontana, A. Monorchio, M. Tosetti, G.L. Tiberi, Estimation of losses in strip and circular wire conductors of radiofrequency planar surface coil by using finite element method, Conc Magn Reson Part B, in press (DOI: 10.1002/cmr.b.21358).
8. J. Jin, Electromagnetic Analysis and Design in Magnetic Resonance Imaging. Boca Raton: CRC, 1999.
9. G. Giovannetti, V. Hartwig, L. Landini, M.F. Santarelli, Sample-induced resistance estimation in Magnetic Resonance experiments: simulation and comparison of two methods, App Magn Res 40 (2011), 351-361.

10. D.I. Hoult, The principle of reciprocity in signal strength calculations - a mathematical guide. Conc Mag Res 12 (2000), 173–187.
11. A. Haase, F. Odoj, M. Von Kienlin, J. Warnking, F. Fidler, A. Weisser, M. Nittka, E. Rommel, T. Lanz, B. Kalusche, M. Griswold, NMR probeheads for in vivo applications, Concepts Magn. Reson. 12 (6) (2000), 361-388.
12. C.E. Hayes, W.A. Edelstein, J.F. Schenck, O.M. Mueller, M. Eash, An efficient, highly homogeneous radiofrequency coil for whole-body NMR imaging at 1.5 T, J Magn Res 63 (1985), 622–628.
13. W.A. Edelstein, G.H. Glover, C.J. Hardy, R.W. Redington, The intrinsic signal-to-noise ratio in NMR imaging, Magn Reson Med 3 (1986), 604–618.
14. V. Hartwig, G. Giovannetti, N. Vanello, L. Landini, M.F. Santarelli, Numerical calculation of peak-to-average Specific Absorption Rate on different human thorax models for Magnetic Resonance safety considerations, App Magn Res 38 (2010), 337-348.
15. T.K.F. Foo, C.E. Hayes, Y.W. Kang, An analytical method for the design of RF resonators for MR body imaging Magn Res Med 21 (1991), 165–177.
16. J. Tropp, Image brightening in samples of high dielectric constant, J Magn Res 167 (2004), 12–24.
17. W.A. Edelstein, T.H. Foster, J.F. Schenck, The relative sensitivity of surface coils to deep lying tissues, in Proceeding of the 4th Annual Meeting of the Society of Magnetic Resonance, London, UK, 964–965 (1985).
18. M.D. Harpen, Sample noise with circular surface coils, Med Phys 14(4) (1987), 616–618.
19. K. Ocegueda, A.O. Rodríguez, A simple method to calculate the signal-to-noise ratio of a circular-shaped coil for MRI, Conc Magn Reson Part A 28A(6) (2006), 422–429.
20. J. Wang, A. Reykowski, J. Dickas, Calculation of the signal-to-noise ratio for simple surface coils and arrays of coils, IEEE Trans Biomed Eng 42 (1995), 908–917.

21. B.H. Suits, A.N. Garroway, J.B. Miller, Surface and gradiometer coils near a conducting body: the lift-off effect, J Magn Reson 135 (1998), 373–379.
22. L.D. Landau, E.M. Lifshitz, Electrodynamics of continuous media – Course of theoretical physics Volume 8. New York: Pergamon Press Limited, 1960.
23. G. Giovannetti, Comparison between circular and square loops for low-frequency magnetic resonance applications: theoretical performance estimation, Conc Magn Reson Part B 46B (2016), 146-155.
24. American Technical Ceramics – Quick reference product selection guide, downloaded at: www.atceramics.com. Accessed December 20, 2017.
25. D. Yeung, J.M.S. Hutchison, D.J. Lurie, An efficient birdcage resonator at 2.5 MHz using a novel multilayer self-capacitance construction technique, Magn Reson Mater Phys Biol Med 3 (1995), 163–168.
26. A. Kumar, W.A. Edelstein, P.A. Bottomley, Noise figure limits for circular loop MR coils, Magn Reson Med 61 (2009), 1201–1209.
27. H.C. Taylor, M. Burl, J.W. Hand, Experimental verification of numerically predicted electric field distributions produced by a radiofrequency coil, Phys Med Biol 42 (1997), 1395–1402

List of captions

Fig. 1 RLC equivalent circuit of a radiofrequency coil

Fig. 2 Circular coil geometry

Fig. 3 MR esperiment simulation

Fig. 4 SNR gain as a function of loop diameter and frequency

Tables

Frequency (MHz)	$R_{coil-strip}$ (mΩ)	$R_{coil-wire}$ (mΩ)	$R_{irr-strip}$ (mΩ)	$R_{irr-wire}$ (mΩ)	R_{cap} (mΩ)	R_{sold} (mΩ)	R_{sample} (mΩ)	ΔSNR (%)
5.7	10.63	6.32	0	0	3	5	0.09473	14.0
21.3	13.77	12.27	0	0	6	10	1.32278	2.5
63.9	25.88	21.33	0.0061	0.0059	20	25	12.2859	2.9
127.8	38.04	30.33	0.0997	0.0977	40	60	49.1438	2.1

Tab. 1 2 cm diameter loop

Frequency (MHz)	$R_{coil-strip}$ (mΩ)	$R_{coil-wire}$ (mΩ)	$R_{irr-strip}$ (mΩ)	$R_{irr-wire}$ (mΩ)	R_{cap} (mΩ)	R_{sold} (mΩ)	R_{sample} (Ω)	ΔSNR (%)
5.7	28.33	15.73	0	0	3	5	0.002214	21.9
21.3	36.26	30.54	0.0029	0.0030	12	10	0.03092	3.4
63.9	68.16	53.45	0.2409	0.2500	30	25	0.28718	1.8
127.8	101.96	77.68	4.1044	4.2616	40	60	1.1487	0.9

Tab. 2 5 cm diameter loop

Frequency (MHz)	$R_{coil-strip}$ (mΩ)	$R_{coil-wire}$ (mΩ)	$R_{irr-strip}$ (mΩ)	$R_{irr-wire}$ (mΩ)	R_{cap} (mΩ)	R_{sold} (mΩ)	R_{sample} (Ω)	ΔSNR (%)
5.7	56.99	31.47	0	0	3	5	0.018977	19.9
21.3	72.92	61.31	0.0468	0.0491	12	10	0.265	1.7
63.9	140.04	109.99	4.0147	4.2093	30	25	2.4611	0.6
127.8	226.33	172.64	77.57	81.285	40	60	9.8443	0.3

Tab. 3 10 cm diameter loop

Frequency (MHz)	$R_{coil-strip}$ (mΩ)	$R_{coil-wire}$ (mΩ)	$R_{irr-strip}$ (mΩ)	$R_{irr-wire}$ (mΩ)	R_{cap} (mΩ)	R_{sold} (mΩ)	R_{sample} (Ω)	ΔSNR (%)
5.7	96.55	47.14	0.0013	0.0013	3	5	0.059145	19.7
21.3	125.17	92.49	0.25	0.25	12	10	0.8259	1.7
63.9	253.56	173.39	23.05	22.91	30	25	7.6707	0.5
127.8	485.43	310.80	570.10	561.03	40	60	30.6828	0.3

Tab. 4 15 cm diameter loop

Supplementary Material

Click here to download Supplementary Material: Sample-coil-rev-marked.doc